Received: 3 April 2019 | Revised: 25 July 2019 | Accepted: 5 October 2019

DOI: 10.1002/suco.201900125

TECHNICAL PAPER

fib CEB-FIP WILEY

Performance of engineered cementitious composites under drop-weight impact: Effect of different mixture parameters

Gürkan Yıldırım[1] | Farhad Emami Khiavi[2] | Özgür Anıl[2] | Oğuzhan Şahin[3] | Mustafa Şahmaran[4] | Recep Tuğrul Erdem[5]

[1]Department of Civil Engineering, Kırıkkale University, Kırıkkale, Turkey

[2]Department of Civil Engineering, Gazi University, Ankara, Turkey

[3]Department of Civil Engineering, Kırşehir Ahi Evran University, Kırşehir, Turkey

[4]Department of Civil Engineering, Hacettepe University, Ankara, Turkey

[5]Department of Civil Engineering, Manisa Celal Bayar University, Manisa, Turkey

Correspondence
Mustafa Şahmaran, Department of Civil Engineering, Hacettepe University, Ankara, Turkey.
Email: sahmaran@hacettepe.edu.tr

Abstract

Current research focuses on the experimental and numerical determination of impact performance of engineered cementitious composites (ECC). Performance assessment of ECC beams with different mixture parameters was made. Mixtures were produced with different replacement rates of Class-F fly ash and slag with Portland cement, water to binder ratios and fiber types (polyvinyl alcohol [PVA] and nylon [N]). Experimental works were validated with incremental dynamic analyses performed by ABAQUS finite element software. Impact testing results were further supported by mechanical property results. Results reveal that each individual mixture parameter used is distinctively effective in modifying the properties under both sudden impact and slow static loading. In brief, enhanced impact resistance is noted when ECC is produced with slag, low amounts of pozzolanic materials, low W/B ratio, fiber addition and PVA fibers. Experimental results were also in line with the numerical results from ABAQUS largely. Significantly, cost-effective N fibers were also shown to be fully replaceable with costly PVA fibers without jeopardizing mechanical/impact performance, if mixture design parameters are adjusted suitably. Current research is likely to attract further research on the development of ECC that is with lower cost and comparable impact/mechanical performance with regards to widely studied more expensive counterparts in the literature.

KEYWORDS

ABAQUS, engineered cementitious composites (ECC), fibers, impact loading, pozzolanic materials

1 | INTRODUCTION

Impact loads which may be caused due to several reasons such as vehicular crash, collisions originated by hurricanes/earthquakes or terror attacks can have severe negative effects on the daily lives of individuals and built environment.[1–3] Therefore, there is a day by day growing awareness among researchers and engineers in designing our infrastructure to be impact resistant.

To improve the impact resistance of reinforced concrete (RC) structures, ideas came along on structural-scale including the changes in structural dimensions and rebar details,[4] utilization of protective barriers around structural components,[5] external strengthening with fiber-reinforced polymer sheets[6] and fiber-RC walls.[7] These ideas, although they are reported to be effective up to certain limits, did not compensate for the drawbacks of conventional concrete

Discussion on this paper must be submitted within two months of the print publication. The discussion will then be published in print, along with the authors' closure, if any, approximately nine months after the print publication.

which has a very brittle nature and very low resistance against impact loading.[8] Structural-scale solutions which are reported to lack in effectively improving the impact resistance of RC structures due to abovementioned drawbacks related to traditional concrete, therefore pushed researchers to seek for alternative solutions on material-scale basis to improve the impact resistance of RC structures.[9]

Due to their unique cracking behavior coupled with enhanced energy absorption capacity/toughness,[10] durability perspectives[11–15] and autogenous self-healing capability,[16–22] engineered cementitious composites (ECC) is becoming more popular to be used in infrastructural construction.[23] Significantly improved tensile strain capacity and modifiable compressive strength levels of ECC make the materials suitable candidates for absorbing impact energy as well.[9,24–26] However, there are certain issues regarding with the mixture compositions of ECC needing to be overcome before widespread applicability of this technology. One of these issues is that ECC do not include coarse aggregates in order not to suffer from fiber balling/clumping and increased matrix fracture toughness significantly reducing the tensile ductility.[27–29] When no coarse aggregates are used in the production of ECC, the amount of Portland cement (PC) increases dramatically which is not desirable in terms of dimensional stability and materials' greenness. To confront these issues, utilization of large volumes of pozzolanic materials (e.g., fly ash [FA], slag) has been a common practice in ECC production.[16,30,31] Another issue related with the mixture compositions of conventional ECC is the presence of specifically tailored (i.e., oil-coated) discrete fibers (e.g., polyvinyl alcohol [PVA] and polyethylene [PE]) which are quite expensive and increase the overall cost of materials.[32] To reduce the increased material costs, research into utilization of cost-effective fibers (e.g., high tenacity polypropylene, natural hemp, and flax fibers) within ECC systems have already started.[33–35] Recently, authors have also concentrated on studies in which cost-effective nylon fibers were used in the production of deflection-hardening High Performance Fiber RCs with large amounts of coarse aggregates.[29,36,37] These studies demonstrated that half of the total volume of costly PVA fibers can be replaced by cheaper nylon fibers without harming basic mechanical properties and causing problems related with restrained shrinkage cracking.

To build on top of former studies performed by the authors and account for the issues related with the mixture proportions of ECC, as explained above, current study mainly focused on the development of new generation ECC mixtures with very high volumes of pozzolanic materials (e.g., Class-F FA and ground granulated blast furnace slag) and cost-effective nylon fibers entirely. Given that the current literature lacks on the related topic, performance characterization of ECC was mainly made by a more elaborated mechanical property of impact resistance together with basic mechanical properties of compressive strength and flexural parameters. Furthermore, experimental results were supported by numerical results obtained from ABAQUS finite element software.

2 | EXPERIMENTAL PROGRAM

2.1 | Materials

The materials used in the production of ECC mixtures were ASTM-compliant CEM I 42.5R ordinary PC, low-lime Class-F FA, ground granulated blast furnace slag (S), silica sand with maximum grain size of 1 mm, water, polycarboxylate-ether-based high range water reducing admixture (HRWRA), PVA and nylon (N) fibers. In Figure 1, gradation curves of PC, FA, S, and silica sand are shown together with their chemical composition/physical properties in Table 1. In Table 2, physical and mechanical properties of different fibers are displayed.

2.2 | Mixture proportions

In total, 36 ECC mixtures were considered in the present study. Mixtures were prepared with two different water to binder (PC + FA or PC + S) ratios (W/B) of 0.27 and 0.35, by weight. To replace PC with high volumes of pozzolanic materials, three different pozzolanic material (FA or S) to PC ratios (FA/PC or S/PC) were selected as 1.2, 2.2, 4.2 and silica sand to binder ratio was constant for all mixtures at 0.36, by weight. Table 3 shows the proportions of mixtures produced. As can be seen from the table, first 12 mixtures were produced without fiber reinforcement and regarded as Control. In 12 of the mixtures numbered from 13 to 24, only N fibers were used by 2% of total mixtures' volume (23 kg/m^3), while in other twelve numbered from 25 to 36, only

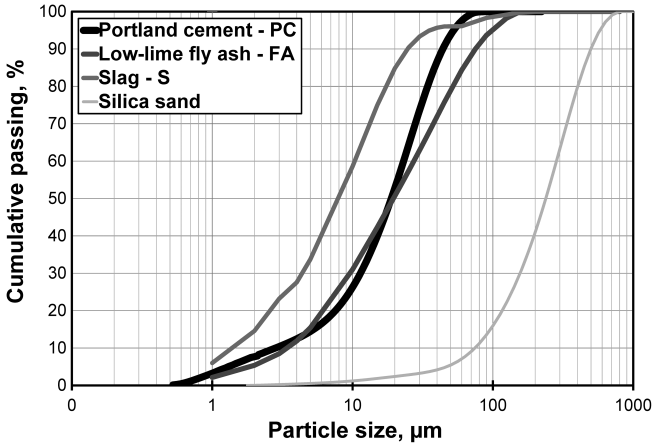

FIGURE 1 Gradation curves of PC, FA, S, and silica sand

PVA fibers were used by 2% of total mixtures' volume (26 kg/m^3). Since the constituents and proportions of different mixtures were different, it was not possible to set a constant amount of HRWRA for all mixtures to achieve identical workabilities. Instead, HRWRA amounts were modified from mixture to mixture to distribute fibers uniformly throughout the matrix with self-consolidating capabilities. Mixtures were named in a way to easily understand their mixture proportions from their designations. For example, 12th mixture which was named as S4.2–0.35 was produced with no fibers, slag, S/B ratio of 4.2 and W/B ratio of 0.35. On the other hand, 26th mixture which was named as FA2.2–P–0.27 was produced with PVA fibers, FA, FA/PC ratio of 2.2 and W/B ratio of 0.27.

TABLE 1 Chemical composition and physical properties of PC, FA, S, and silica sand

Chemical composition	PC	FA	S	Silica sand
CaO	61.43	3.48	35.09	0.02
SiO_2	20.77	60.78	37.55	99.79
Al_2O_3	5.55	21.68	10.55	0.06
Fe_2O_3	3.35	5.48	0.28	0.02
MgO	2.49	1.71	7.92	0.01
SO_3	2.49	0.34	2.95	—
K_2O	0.77	1.95	1.07	0.01
Na_2O	0.19	0.74	0.24	0.02
Loss on ignition	2.20	1.57	2.79	0.07
$SiO_2 + Al_2O_3 + Fe_2O_3$	29.37	87.94	48.38	99.87
Physical properties				
Specific gravity	3.06	2.10	2.79	2.60
Blaine fineness (m^2/kg)	325	269	425	—

Abbreviations: FA, fly ash; PC, Portland cement.

2.3 | Preparation of specimens

To be used in different tests, specimens were manufactured from a single batch for each mixture. Identical mixing procedures were followed for all of the proposed mixtures. During mixing, first, PC, FA, or S and silica sand were first mixed in dry state. Then, water and HRWRA were slowly added to the previously stirred blend of dry constituents. For mixtures with fiber reinforcement, as the final step, discrete fibers were slowly added to the fresh mixture and mixed at high speed until dispersed homogenously.

To be used in impact testing, for each mixture, two beam specimens without any continuous steel reinforcement measuring 50 × 50 × 750 mm^3 were cast. In addition, for each mixture at least three separate cubic specimens with dimensions of 50 mm were cast to be used in compressive strength testing, along with four separate smaller beam specimens measuring 50 × 75 × 360 mm^3 for measuring the flexural parameters (i.e., flexural strength and displacement). After the completion of casting of fresh mixtures into the molds, the surfaces of all specimens were covered with plastic sheets and kept in laboratory medium at 50 ± 5% relative humidity (RH) and 23 ± 2°C for 24 hr. After removed from their molds with the completion of 24 hr, specimens were placed and cured in impermeable plastic bags for additional 27 days where the environmental conditions were set at 95 ± 5% RH and 23 ± 2°C.

2.4 | Testing and instrumentation

Compressive strength testing was performed with the help of compression device which applied uniaxial loading on

TABLE 2 Physical and mechanical properties of different fibers

Type of fiber		Length (mm)	Diameter (mm)	Tensile strength (MPa)	Modulus of elasticity (GPa)	Specific gravity
PVA		8	0.039	1,092	42.8	1.30
N		19	0.050	966	25.0	1.14

Abbreviations: N, nylon; PVA, polyvinyl alcohol.

TABLE 3 Weights of constituents of different mixtures and 28-day basic mechanical property results

		Constituents (kg/m^3)								28-Day mechanical properties		
								Fibers				
Mixture #	Mixture ID.	PC	FA	S	Silica sand	Water	HRWRA	PVA	N	Compressive strength, (MPa)	Flexural strength (MPa)	Flexural displacement (mm)
1	FA1.2–0.27	575	690	—	458	342	5.0	—	—	50.5	4.6	0.3
2	FA2.2–0.27	389	856	—	444	336	3.8	—	—	32.6	5.5	0.4
3	FA4.2–0.27	235	987	—	444	330	1.3	—	—	17.8	3.1	0.3
4	FA1.2–0.35	522	626	—	417	402	4.5	—	—	49.3	3.7	0.4
5	FA2.2–0.35	353	777	—	409	395	3.2	—	—	16.6	3.4	0.3
6	FA4.2–0.35	214	899	—	405	390	0.8	—	—	13.2	2.5	0.2
7	S1.2–0.27	607	—	728	475	361	6.0	—	—	80.2	5.6	0.3
8	S2.2–0.27	414	—	911	476	358	4.5	—	—	62.9	6.3	0.3
9	S4.2–0.27	253	—	1,063	477	355	3.2	—	—	48.0	6.1	0.3
10	S1.2–0.35	548	—	658	431	422	5.1	—	—	61.6	4.9	0.4
11	S2.2–0.35	375	—	825	426	420	4.0	—	—	50.2	5.0	0.3
12	S4.2–0.35	229	—	962	430	417	2.7	—	—	33.7	5.3	0.3
13	FA1.2–N–0.27	563	676	—	451	334	5.0	—	23	54.6	4.8	1.9
14	FA2.2–N–0.27	380	836	—	442	328	3.8	—	23	45.9	5.8	2.6
15	FA4.2–N–0.27	231	970	—	428	324	1.3	—	23	33.8	3.8	2.9
16	FA1.2–N–0.35	512	614	—	407	394	4.5	—	23	50.4	4.5	3.9
17	FA2.2–N–0.35	346	761	—	400	387	3.2	—	23	25.9	5.2	5.4
18	FA4.2–N–0.35	210	882	—	394	382	0.8	—	23	18.4	3.6	5.4
19	S1.2–N–0.27	595	—	714	465	353	6.0	—	23	85.6	7.2	1.0
20	S2.2–N–0.27	405	—	891	470	350	4.5	—	23	63.8	6.9	1.0
21	S4.2–N–0.27	248	—	1,042	467	348	3.2	—	23	56.4	6.8	1.1
22	S1.2–N–0.35	536	—	643	426	413	5.1	—	23	69.3	5.3	2.1
23	S2.2–N–0.35	366	—	805	426	410	4.0	—	23	57.6	6.3	1.9
24	S4.2–N–0.35	225	—	945	416	409	2.7	—	23	37.4	6.2	1.7
25	FA1.2–P–0.27	563	676	—	451	334	5.0	26	—	60.9	9.5	1.5
26	FA2.2–P–0.27	380	836	—	442	328	3.8	26	—	48.2	9.1	1.6
27	FA4.2–P–0.27	231	970	—	428	324	1.3	26	—	35.0	7.4	3.2
28	FA1.2–P–0.35	512	614	—	407	394	4.5	26	—	56.3	8.8	2.5
29	FA2.2–P–0.35	346	761	—	400	387	3.2	26	—	30.9	8.6	3.2
30	FA4.2–P–0.35	210	882	—	394	382	0.8	26	—	23.3	6.2	3.5
31	S1.2–P–0.27	595	—	714	465	353	6.0	26	—	87.1	11.4	1.1
32	S2.2–P–0.27	405	—	891	470	350	4.5	26	—	69.4	11.0	1.4
33	S4.2–P–0.27	248	—	1,042	467	348	3.2	26	—	58.6	12.6	1.1
34	S1.2–P–0.35	536	—	643	426	413	5.1	26	—	73.3	11.2	1.7
35	S2.2–P–0.35	366	—	805	426	410	4.0	26	—	63.8	10.9	1.5
36	S4.2–P–0.35	225	—	945	416	409	2.7	26	—	41.3	11.9	2.4

Abbreviations: FA, fly ash; HRWRA, high range water reducing admixture; N, nylon; PC, Portland cement; PVA, polyvinyl alcohol.

50 mm cubic specimens at a rate of 0.9 kN/s. For the determination of flexural parameters, a universal testing device equipped with a data acquisition system was used to apply loading under four-point bending. Flexural loading was applied on a span length of 304 mm and a central span length of 101 mm at a rate of 0.005 mm/s. While calculating

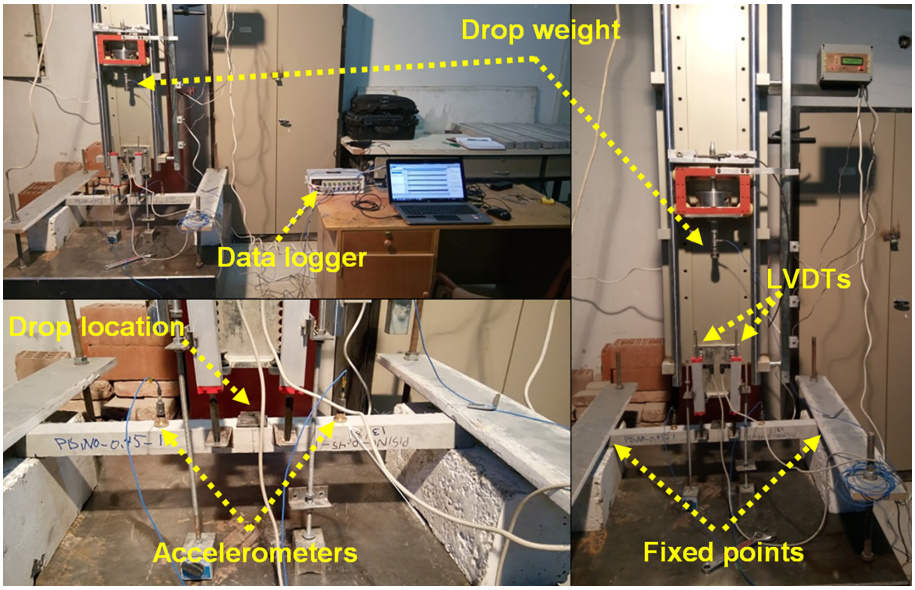

FIGURE 2 Free fall drop-weight test setup

the flexural strength, maximum level of flexural loading level was taken into account. Midspan beam displacement was correspondent to that of maximum level of flexural loading similar to calculation of flexural strength.

During impact testing, free fall drop-weight test setup shown in Figure 2 was used. Selection of the test setup was based on a previous collaborative work of the authors[24] where the same test setup was used for the impact performance analysis of different concrete grades, specimen dimensions and impact energies was made and no adverse effects (e.g., settlement, embedment etc.) regarding the support conditions were reported. Test setup was specifically designed to permit free falling of objects with different weights from a maximum height of 2.5 m onto the specimens. Both ends of $50 \times 50 \times 750$ mm^3 beam specimens were prepared to work as a fixed support. To achieve the fixed support conditions, specimens were placed on high-strength concrete blocks with 30 mm equal support lengths from both sides. After, wooden plates were placed on top of the specimens which were then squeezed with the help of a bolt-nut system and fixed to the ground. No embedment or damage occurred in the high-strength concrete blocks used as supports during the impact tests. All impact tests were made by considering identical geometry of impacting edge, drop weight, and height. A 9 kg hammer was dropped from a height of 60 cm on the same point to exert impact loading on beam specimens. With the purpose of achieving a distributed loading and preventing local failures, a high strength steel plate measuring $50 \times 50 \times 4$ mm^3 which was fixed to the specimens by a mechanical anchor was placed on the point of impact for each beam specimen. In order not to be affected by the localization of impact loading due to surface irregularities of specimens, a rubber piece was placed between the plates and specimens. Level of impact loading was 52.97 J (600 mm $\times$ 9.81 m/s^2 $\times$ 9.0 kg [height of drop weight $\times$ gravitational acceleration $\times$ mass of drop weight]). During impact testing, accelerations from symmetrical sides of beams were measured with the help of two separate accelerometers 150 mm aside from the impact point. Two linear variable displacement transducers placed 50 mm aside from the impact point were benefited while recording displacement values of beams after impacted (Figure 2). The loading created by the drop hammer was measured using a dynamic load cell. Impact velocity of the drop hammer was calculated by a speedometer placed on top of the hammer, and average measured impact velocities of beam specimens were 4.29 m/s. More detailed explanations regarding with the experimental setup of impact loading and selection of proposed testing parameters can be found in Banyhussan et al.[37]

3 | RESULTS AND DISCUSSION

3.1 | Basic mechanical properties

Main aim of the current research is to concentrate on the impact behavior of ECC mixtures manufactured with new design parameters. Therefore, only general discussions of basic mechanical properties were presented to have an understanding on the overall behaviors of different mixtures. Under this title, compressive strength, flexural strength, and midspan beam displacement results were discussed by taking the average values listed in Table 3 into consideration. Average results were evaluated considering the variant mixture parameters including W/B ratios, FA/PC, or S/PC ratios and inclusion/types of different fibers into ECC mixtures.

3.1.1 | Compressive strength

Compressive strength results clearly decreased with the increase of W/B ratios of specimens and the rates of decrement varied depending on the mixture proportions. This was a very likely outcome and attributed to increased contents of water in the cementitious mixtures. With the increase of W/B ratio from 0.27 to 0.35, nearly 60 kg more water per cubic meter of concrete was added to the mixtures which expectedly lowered the compressive strength. When the amount of pozzolanic materials was increased in the mixture compositions of ECC, considerable reductions in the average compressive strength results were noted, irrespective of other mixture parameters (Table 3). This was due to significantly lowered PC amounts in the presence of high volumes of pozzolanic materials retarding hydration reactions and strength gain. Depending on the type of pozzolanic materials, compressive strength results changed as well. When other parameters were kept the same, slag-bearing specimens resulted in relatively higher compressive strength results. For example, average compressive strengths of FA4.2–P–0.27 and S4.2–P–0.27 mixtures were 35.0 and 58.6 MPa, respectively. This was due to significantly higher self-cementing capability of slag particles compared to Class-F FA used in the study which was relatively pozzolanic.[16] Fiber addition into control mixtures numbered from 1 to 12 in Table 3, caused compressive strength results to increase slightly. This was attributed to the effects of micro-size fibers in delaying crack formation and arresting flaws at microlevels. Rates of increment with the fiber inclusion were variant and they seemed to be not as influential as other mixture parameters (FA or S/PC ratio and W/B ratio) in general.

3.1.2 | Flexural strength

Increasing W/B ratio of mixtures lowered the flexural strength results. When the utilization rate of pozzolanic materials within the mixtures was increased, majority of flexural strength results decreased considerably. Moreover, the type of pozzolanic materials was also very influential on the flexural strength test results. In most of the cases, ECC produced with slag resulted in higher flexural strength results. In general sense, flexural strength results followed a trend similar to that of compressive strength results with the tested mixture parameters since the factors influencing compressive strength results are also generally effective on flexural strength results. However, fiber addition/types made more significant changes in flexural strength results of control mixtures in comparison to compressive strength results. For example, average flexural strength result of S1.2–0.27 mixture increased by 29 and 104% when the mixture was incorporated with N (from 5.6 to 7.2 MPa) and P (from 5.2 to 11.4 MPa) fibers, respectively. Similar modality was also observable for mixtures with different variant parameters. The reason for flexural strength results to be affected more than compressive strength results with the fiber inclusion can be in relation with more elaborated factors (e.g., tensile first cracking strength, ultimate tensile strength, and tensile strain capacity), especially when materials are characterized by strain/deflection-hardening response.[16,38] Additionally, PVA fibers were better in terms of improving the flexural strength results compared to N fibers (Table 3). This might be associated with the comparably higher elastic modulus of PVA fibers (42.8 GPa) compared to N fibers (25 GPa).[39]

3.1.3 | Midspan beam displacement

Average midspan beam displacement results which represent the overall ductility of cementitious composites are shown in Table 3. In addition, in Figure 3, flexural strength—midspan displacement plots of specimens obtained from different mixtures were presented for comparison.

When the W/B ratio of mixtures was increased, considerable increments in the ductility of mixtures was noted and this behavior was very evident for fiber reinforced mixtures (Table 3, Figure 3). This can be related with the reduced amounts of total cementitious materials which also reduce the chance for individual fibers to chemically bond to the cementitious matrices.[40] Similarly, general ascending trend in displacement results was noted with the increased rates of pozzolanic materials in mixtures when other mixture parameters were the same. This trend was significantly clearer for mixtures with FA (due to spherical morphology of particles improving the fiber distribution and reducing matrix fracture toughness) rather than mixtures with slag. This finding was also related with the changes in the interface properties of cementitious composites with different pozzolanic materials and individual cement replacement materials in modifying fiber distribution and matrix fracture toughness of ECC.

Fiber inclusion into control mixtures significantly favored the overall ductility of ECC mixtures irrespective of other mixture parameters (Table 3, Figure 3). This was a very sensible outcome considering the effects of fibers in delaying cracking formation and bridging individual crack openings. However, it needs to be stated that not all of N fiber-reinforced mixtures were characterized with deflection-hardening response, although comparable levels of midspan displacement were recorded. Deflection-hardening behavior is confirmed if the peak load and its corresponding midspan beam displacement are greater than the first cracking load and its corresponding midspan displacement at first cracking

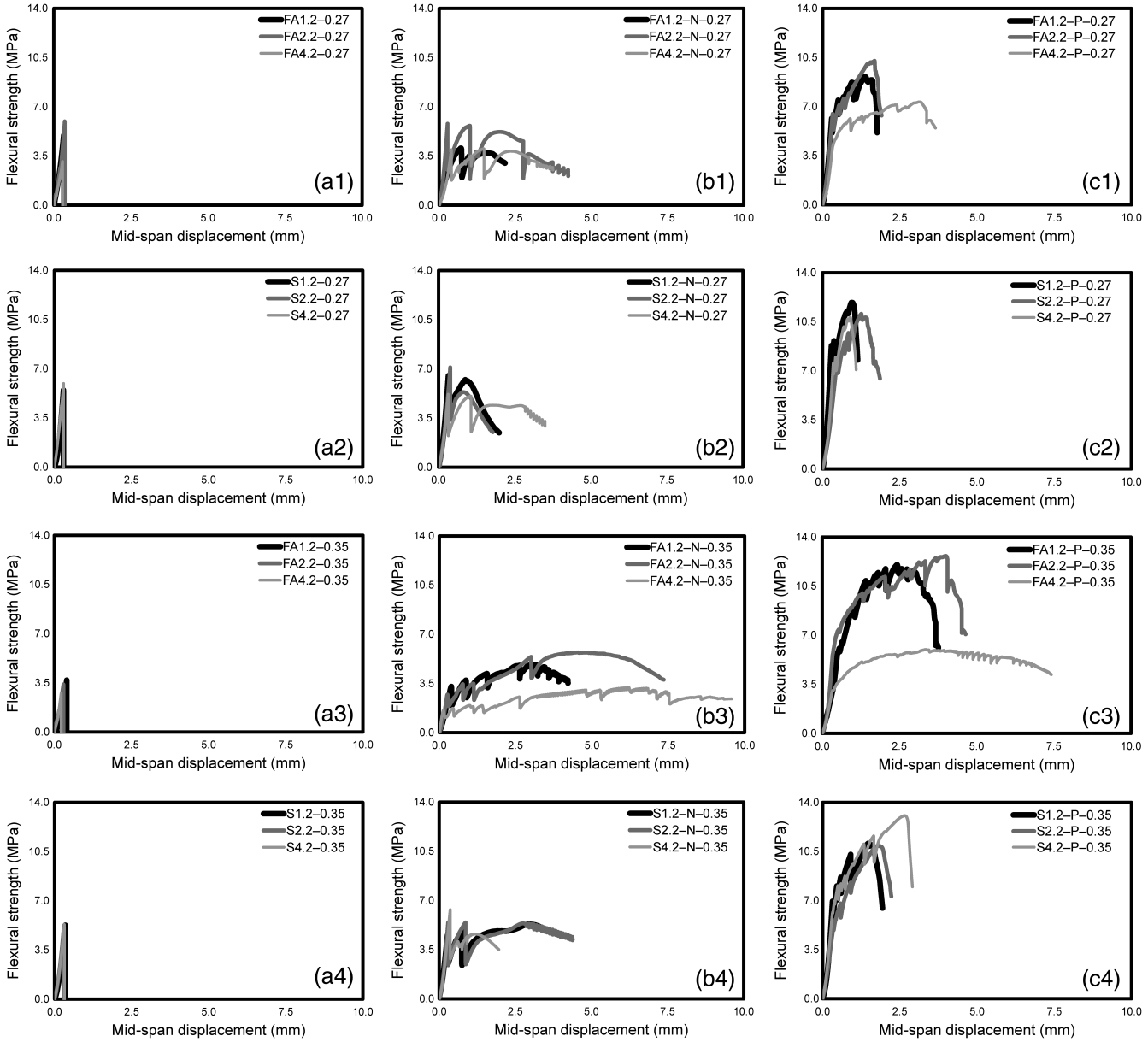

FIGURE 3 Plots of flexural strength—midspan displacement graphs for specimens with different mixture parameters

load, respectively. Deflection-hardening response can be further improved when the gap between the first cracking load/peak load and deflection at the first cracking load/deflection at the peak load is increased.[41] Based on the abovementioned explanations regarding with the definition of deflection-hardening response, it can be stated that regardless of the different mixture parameters, specimens incorporated with PVA fibers exhibited deflection-hardening response, although this was not the case for specimens with N fibers all the time. As can be followed from Figure 3, the response of specimens produced with N fibers was variant and depending on the different mixture design parameters it was possible to obtain either deflection-softening or deflection-hardening response under four-point bending. For example, when N fiber incorporated mixtures were prepared with FA rather than slag and with W/B ratio of 0.35 rather than 0.27, deflection-hardening response was achievable for all FA utilization rates (Figure 3), although the extent of flexural strength and midspan displacement were lower compared to specimens with PVA fibers. It should be kept in mind that the mixtures were produced with fibers on a volumetric basis (2% of total mixtures' volume) which resulted in differences in fiber amounts for different mixtures (26 kg/m^3 for PVA-based and 23 kg/m^3 for N-based mixtures) due to the differences in specific gravities of PVA and N fibers. Therefore, at identical fiber amounts per cubic meter of concrete, more alike mechanical behaviors are very likely to be obtained from specimens with PVA and N fibers. However, basic

TABLE 4 Free fall drop-weight impact test results

Mixture		Acceleration—g (m/s^2)							
		Left		Right		Displacement (mm)			
#	ID.	Max.	Min.	Max.	Min.	Left	Right	Residual displacement (mm)	Impact load (kN)
1	FA1.2–0.27	141.0	−18.7	140.6	−132.1	43.9	44.0	44.0	13.0
2	FA2.2–0.27	90.8	−64.6	88.9	−26.7	58.8	58.6	58.8	13.1
3	FA4.2–0.27	61.3	−57.1	60.1	−22.2	75.0	74.5	75.0	13.0
4	FA1.2–0.35	88.8	−18.4	86.9	−38.8	55.2	55.1	55.2	13.0
5	FA2.2–0.35	54.0	−47.4	53.8	−20.5	71.2	72.0	72.0	13.1
6	FA4.2–0.35	45.0	−31.2	44.0	−28.9	90.3	90.1	90.3	13.0
7	S1.2–0.27	196.1	−170.2	195.1	−126.1	34.7	34.5	34.7	13.3
8	S2.2–0.27	163.9	−117.2	163.1	−62.1	43.6	42.9	43.6	13.0
9	S4.2–0.27	140.3	−27.1	138.1	−57.3	59.1	58.9	59.1	13.2
10	S1.2–0.35	127.0	−127.0	126.8	−43.0	52.3	51.7	52.3	13.1
11	S2.2–0.35	115.3	−73.9	115.7	−67.2	59.4	59.7	59.7	13.1
12	S4.2–0.35	90.7	−89.8	91.0	−40.1	81.5	81.8	81.8	13.0
13	FA1.2–N–0.27	162.5	−197.1	161.3	−307.3	24.4	22.6	15.3	13.2
14	FA2.2–N–0.27	105.7	−162.6	101.5	−23.6	33.3	29.3	23.7	12.6
15	FA4.2–N–0.27	71.4	−44.7	70.0	−44.3	41.8	47.4	30.6	13.2
16	FA1.2–N–0.35	102.9	−88.6	104.1	−100.0	32.8	32.0	21.8	13.5
17	FA2.2–N–0.35	63.1	−32.1	64.0	−32.7	47.5	46.7	27.3	13.0
18	FA4.2–N–0.35	52.1	−13.4	51.1	−14.5	54.4	54.1	36.7	13.0
19	S1.2–N–0.27	225.0	−107.8	225.9	−111.4	18.9	17.3	13.6	13.1
20	S2.2–N–0.27	188.8	−78.5	187.5	−133.0	22.9	22.5	22.4	13.2
21	S4.2–N–0.27	162.0	−97.7	160.2	−126.2	30.0	29.9	24.1	13.1
22	S1.2–N–0.35	146.6	−70.2	148.0	−42.4	26.7	26.3	16.7	13.1
23	S2.2–N–0.35	119.6	−46.0	118.5	−79.7	28.2	28.9	24.3	13.0
24	S4.2–N–0.35	110.0	−79.8	112.8	−65.3	37.0	37.6	27.0	13.0
25	FA1.2–P–0.27	186.6	−116.1	185.2	−165.7	19.6	20.0	12.0	13.2
26	FA2.2–P–0.27	148.8	−131.4	147.0	−113.2	26.4	25.9	17.4	13.1
27	FA4.2–P–0.27	115.8	−38.9	114.6	−114.4	35.3	35.0	25.8	13.1
28	FA1.2–P–0.35	121.4	−109.7	121.2	−66.9	28.2	28.7	18.6	13.0
29	FA2.2–P–0.35	96.7	−85.7	94.8	−70.9	38.0	37.8	27.0	13.4
30	FA4.2–P–0.35	74.6	−74.7	74.1	−56.0	49.7	50.6	29.5	13.4
31	S1.2–P–0.27	255.7	−234.8	254.4	−141.6	17.5	15.2	10.8	13.1
32	S2.2–P–0.27	200.5	−197.2	197.9	−176.6	20.2	20.8	16.4	13.2
33	S4.2–P–0.27	167.1	−164.5	164.8	−158.2	27.4	26.1	20.0	13.1
34	S1.2–P–0.35	165.1	−145.6	164.9	−108.2	24.2	24.5	14.9	13.0
35	S2.2–P–0.35	130.9	−76.0	128.6	−118.4	26.4	27.0	22.1	13.1
36	S4.2–P–0.35	115.1	−86.4	113.6	−99.5	34.7	34.8	25.8	13.1

mechanical property results show that, even when less amounts of fibers are used, ECC mixtures produced with N fibers can be designed to achieve performance similar to mixtures produced with PVA fibers through proper controlling of other design parameters (i.e., W/B ratio, type and amount of pozzolanic materials).

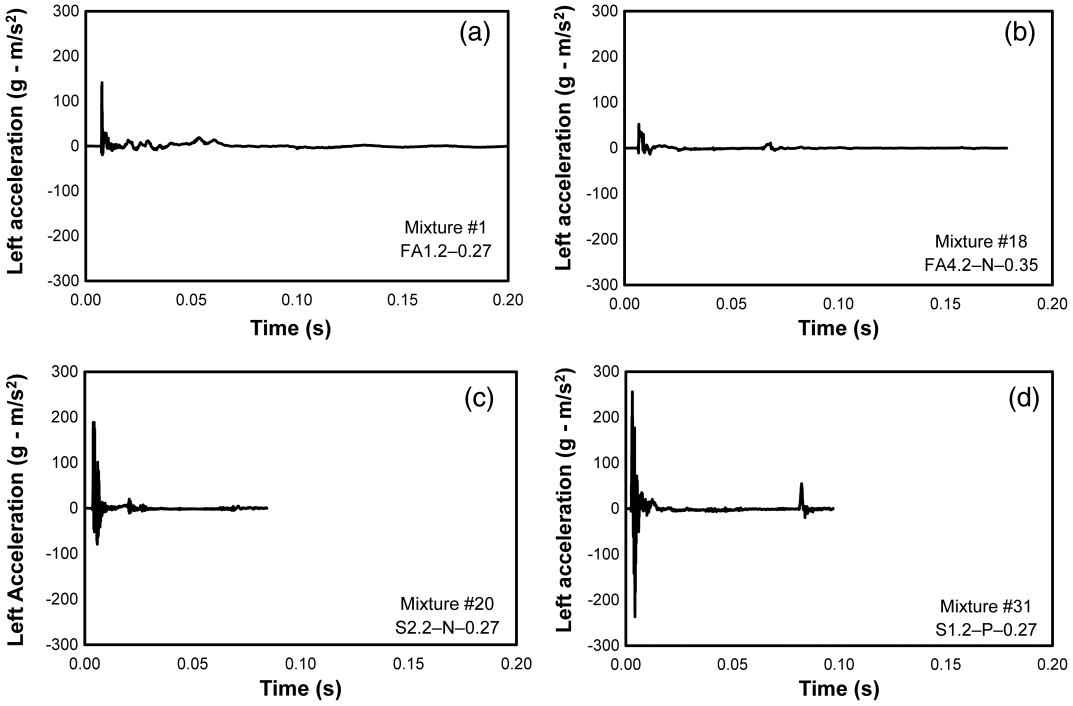

FIGURE 4 Representative acceleration versus time graphs for selected mixtures

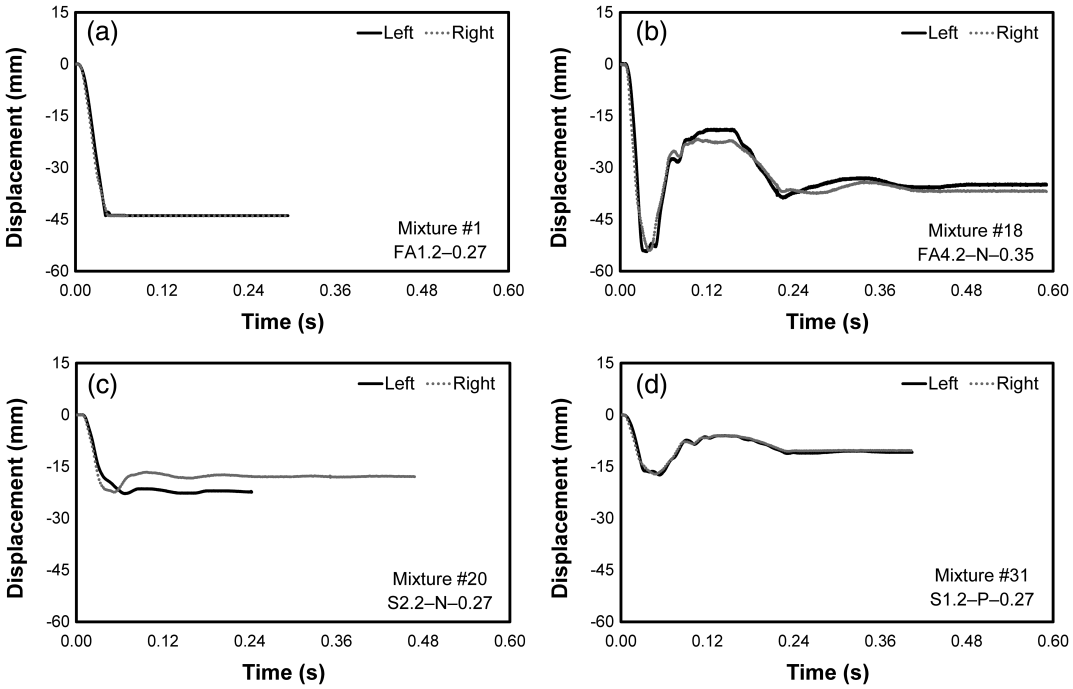

FIGURE 5 Representative displacement versus time graphs for selected mixtures

3.2 | Impact behavior

Table 4 shows the results obtained after the implementation of impact tests on specimens from different mixtures. The results were evaluated in terms of acceleration, displacement, and residual displacement values. Some selected examples of acceleration versus time, displacement versus time and impact load versus time graphs are shown in Figures 4–6, respectively. As can be followed from Table 4, there were natural scattering on the applied impact loads on different specimens due to nature of impact testing and heterogeneous nature of tested concrete specimens, although

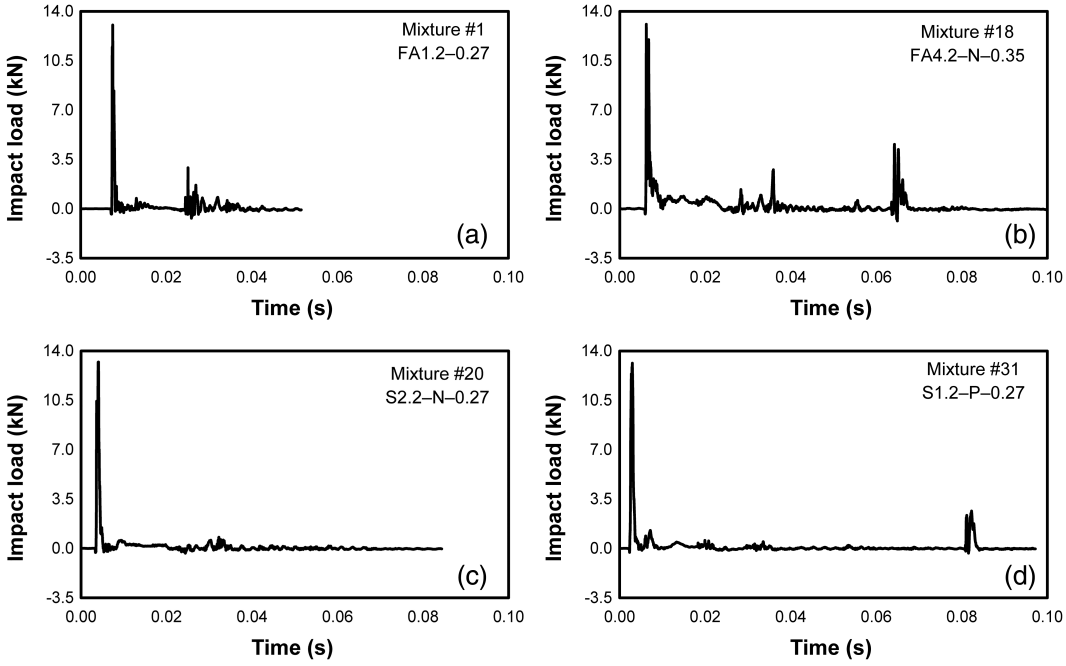

FIGURE 6 Representative impact load versus time graphs for selected mixtures

FIGURE 7 Representative photos showing the effects of (a) type and (b) amount of pozzolanic materials on impact response of ECC

these were relatively limited. Impact loads ranged between the values of 12.5 and 13.5 kN and mostly stayed in the range of 13.0 kN meaning that all specimens were subjected to relatively similar loading conditions and the test setup was consistent. Below, impact resistance of different ECC mixtures was assessed in detail by focusing specifically on the variant parameters of the experimental work: that is, effect of utilization of different types/amounts of pozzolanic materials, effect of water to binder ratio, and effect of utilization of different fiber types.

3.2.1 | Effect of utilization of different types/amounts of pozzolanic materials

There was a clear sight regarding the effects of utilization of different types and amounts of pozzolanic materials on the impact behavior of ECC mixtures. As seen from Table 4 and represented photos of impacted specimens in Figure 7a, specimens of slag-bearing mixtures resulted in increased maximum acceleration, decreased midspan displacement and residual displacement results compared to those bearing FA, when other mixture parameters were the same. To safely endure impact loads, concrete needs to have adequate strength both in compression and tension.[9,37] This is important because, when impacted, the frontal face of concrete which is in direct contact with the introduced impact energy is subjected to compressive stress waves while the free distal face at the back is subjected to tensile stress waves which are reflected as a result of the introduction and progression of compressive stress waves. Adequate levels of compressive and tensile strength are therefore important for concrete not to crush/fail from the frontal and distal faces, respectively. Increased ductility provides additional benefits to composites in uniformly distributing the created impact deformation and maintaining the overall integrity of the material.[37] Based on above discussions, a plausible explanation for increased impact performance of specimens with slag can be in relation with significantly higher compressive strength results (Table 3). It can also be inferred from the above discussions that among other parameters being influential on impact performance of concrete materials, adequate compressive strength seems the most crucial and basic one, because, in cases where the material itself is not with adequate compressive strength, failure takes place from the frontal face of the specimen and there is no further capability to sustain and distribute the damage through increased flexural strength and ductility (see below).

When higher utilization rates of different types of pozzolanic materials were targeted in mixture proportions, significant reductions in impact resistance of specimens (as reflected especially by increased displacement results) were monitored (Table 4, Figure 7b). FA-incorporating specimens influenced more by the increased utilization rates compared to slag-incorporating specimens. For example, percental increments in average of left and right displacement results presented in Table 4 were noted to be 33% (from 23.5 to 31.5 mm) and 90% (from 23.5 to 44.6 mm) for FA2.2–N–0.27 and FA4.2–N–0.27 mixtures with respect to FA1.2–N–0.27 while similar increments were 25% (from 18.1 to 22.7 mm) and 65% (from 18.1 to 30.0 mm) for S2.2–N–0.27 and S4.2–N–0.27 mixtures with respect to S1.2–N–0.27, respectively. Despite significant increments in ductility (midspan displacement) results of specimens in the presence of higher replacement rates of pozzolanic materials (Table 3), reductions in the impact resistance of specimens clearly show the paramount importance of necessity to reach adequate compressive and relatedly tensile strength levels to prevent failure from the first impact zone and improve impact resistance.

3.2.2 | Effect of different water to binder ratios

Changes in the impact performance of ECC mixtures with different water to binder ratios (W/B) were evident from Table 4. According to the results presented in Table 4 and selected representative photos of impacted specimens (Figure 8), clear reductions in the measured acceleration and increments in displacement results were noted when W/B ratio of all mixtures were increased from 0.27 to 0.35 and other mixture parameters were identical. For example, after impacted, the residual displacement results for S1.2–P–0.27, S2.2–P–0.27, and S4.2–P–0.27 mixtures were 10.8, 16.4, and 20.0 mm while the results increased by 38, 35, and 29% reaching to 14.9, 22.1, and 25.8 mm levels for S1.2–P–0.35, S2.2–P–0.35, and S4.2–P–0.35 mixtures, respectively. Similar trend was observed for rest of mixtures irrespective of other mixture parameters. The most probable reason for the reduced impact resistance of ECC mixtures at higher W/B

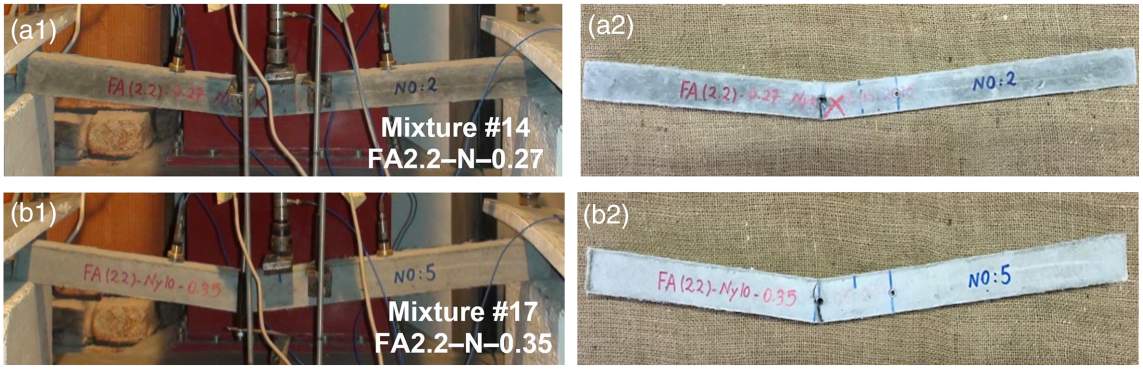

FIGURE 8 Representative photos showing the effect of W/B ratio on impact response of ECC

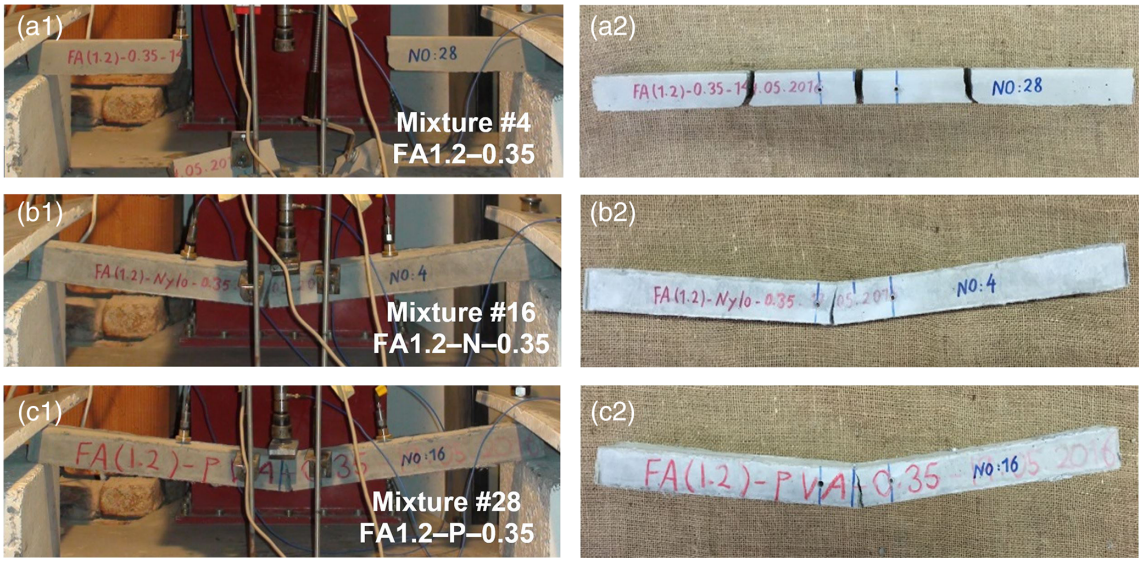

FIGURE 9 Representative photos showing the effects of utilization and type of fibers on impact response of ECC

ratios can be in relation with the considerably reduced compressive strength results which brings about even lower tensile strength results causing direct and sudden failure of specimens in the incident of impact. This finding is also in line with several studies in the literature which state that increments in compressive strength significantly improve the impact resistance of concrete.[24,42–44]

According to studies available in the literature, however, results contradictory to what was observed herein were also reported especially for concrete mixtures reinforced with different types of fibers having higher W/B ratios. It was previously concluded that for fiber RC mixtures, higher levels of impact energy were absorbed at higher water to cement ratios and this response was mostly related to the properties of interface between the cementitious matrices and individual fibers.[45] When the water to cement ratio is high, the matrix strength decreases creating weaker interfacial bonding between the fibers and the matrix compared to counterpart mixtures with low water to cement ratio. In the incident of impact loading which is relatively sudden, this may cause individual fibers to easily slip out without absorbing too much energy instead of being pulled out followed by rupturing.[45] Although this is a plausible statement, this behavior observed at higher levels of water to cement ratios, is likely to be affected by numerous factors such as the impact testing setup, size of specimen tested, drop height, and alignment/type/amount of fibers.[46] As a consequence, it is therefore suggested that these parameters, especially those related to the materials' characteristics should be optimized in a way to obtain higher impact energy absorption capacities by modifying matrix strength and fiber properties which would allow the pulling out of fibers rather than direct rupturing when the specimens are impacted.

3.2.3 | Effect of utilization and types of fibers

Addition of discrete discontinuous fibers into control mixtures numbered from 1 to 12 led substantial improvements in the impact performance of mixtures regardless of the type/amount of pozzolanic materials, W/B ratios and fiber types. To exemplify, average of measured left and right displacements for FA1.2–0.27 mixture (44 mm) was improved by 87 and 122% decreasing down to levels of 15.3 and 12 mm when the same mixture was incorporated with N and PVA fibers, respectively. This general trend was in line with the related studies available in the literature.[47–49]

The major contribution of fibers is to keep the overall integrity of concrete material after subjected to impact loading through restraining the propagation/distribution of cracks and consequently crater formation (Figure 9). As briefly mentioned previously, tensile strength is as important as the compressive strength for a specimen subjected to sudden impact effect since compressive waves created right after the introduction of impact loading at the frontal face would be experienced as tensile waves as a result of reflection from other free surfaces of the tested specimen.[9,37] The train of originally created compressive waves is interrupted with the formation of tensile waves. As a result, an algebraic summation of tensile and compressive waves form with compressive waves losing intensity from the source of impact towards rest of free surfaces and tensile waves gaining intensity after reflected from free surfaces back to the initially impacted surface. If the stresses created either by tensile or compressive waves exceed the corresponding strengths at specific locations, damage takes place and the possibility for damage to occur continues until the dampening of resultant stress below the strength of material tested.[47] Considering the fact that tensile strength of concrete is at a fraction of

compressive strength, the governing criterion for the impact resistance is mostly tensile strength.[50] In line with the above statements, improvement of flexural impact performance of mixtures produced in this study can be in relation with the enhanced flexural strength and midspan beam displacement capacity of specimens (as evidenced from Table 3 and Figure 3) in the presence of fibers. Here, the improvement of flexural strength accounts for the extent of damage experienced and midspan beam displacement (i.e., ductility) helps arresting and even distribution of resultant damage in favor of keeping the tested specimen in one piece.

Fibers also help improve the energy absorption capacity of control mixtures. As can be seen from the Figure 3, toughness (area under the plastic region of flexural strength-displacement plot) values of specimens got substantially larger with the utilization of different types of fibers. Moreover, more pronounced deflection-hardening response further contributes to the enlargement of toughness area and relatedly improved impact resistance of tested specimens. This argument was also made in the studies of Mao et al.[48] and Barnett et al.[49] who tested the blast resistance of fiber-reinforced ultrahigh performance concrete (FR-UHPC) slabs and concluded that increased postcracking tendency and deflection-hardening response (obtained from some of the specimens) result in high flexural energy absorption capacity for FR-UHPC specimens. In addition, in a previous study, improved flexural strength (one of the parameters contributing to higher deflection-hardening capacity) was reported to reduce the diameter of crater formed as a result of projectile impact[51] which was also the case in this study. Furthermore, the impact resistance of control mixtures is likely to be improved as a result of increments in the compressive strength results with the inclusion of fibers (Table 3). Higher levels of compressive strength may contribute to the damping of impact loading at the initial point of impact which may also relive the reflected tensile impact energy at the distal face and lead to increased impact resistance.[51]

As one of the main aims of the current study was to see the possibility of replacing costly PVA fibers with relatively cheaper N fibers, impact performance was also evaluated in terms of contribution of different fiber types to the impact resistance. As can be followed from Table 4, at a constant pozzolanic material utilization rate and W/B ratio, mixtures incorporated with PVA fibers gave lower displacement results compared to mixtures with N fibers after impacted, although the differences were mostly very small. Slightly better performance of PVA fibers in enhancing the impact resistance of ECC can be associated with several reasons: (a) higher tensile strength and modulus of elasticity of PVA fibers (Table 2) are likely to lead to a tougher impact response; (b) better improvements in flexural strength and displacement capacity of specimens contribute to the enlargement of toughness area; (c) due to higher specific gravity, for constant 2% of total mixtures' volume, PVA fibers weigh more (26 kg) than N fibers (23 kg) per cubic meter of concrete; and (d) length and diameter of PVA fibers are considerably less than N fibers meaning that they will be available in greater numbers for a specified concrete space. Moreover, a previous study revealed that concrete produced with shorter fibers and subjected to projectile impact resulted in crater with smaller diameter.[51] A possible explanation for the better impact performance of concretes with shorter fibers (as in the case of PVA fiber-based ECC here) could be that if the fibers were oriented at an angle to the loading and/or impact direction, those with longer lengths are expected to be under local bending around the crack which creates flexural and compressive stresses in fibers and matrix itself, respectively. This means that larger area will be disturbed in the matrices of concretes produced with longer fibers creating greater damage.[51]

Despite their lower amount of usage compared to PVA fibers per cubic meter, utilization of N fibers greatly contributed to the impact resistance of ECC so that results that were close to PVA fiber-based composites were acquired (Table 4). Fibers with higher tensile strength transfer higher tensile stresses from the cementitious matrix to the fibers.[52] Although the tensile strength of PVA fibers (1,092 MPa) is higher than that of N fibers (966 MPa), the possible reactions between the mixing water and amide chains (—CO—NH—) of N fibers may partly play a role in enhancing the capacity of N fibers to resist in additional tensile stresses. Upon contact with water, bonding takes place between the oxygen in water and hydrogen on nitrogen and between the hydrogen in water and oxygen on carbon. As moisture is absorbed and bonds to the polymer backbone, the nylon swells.[53,54] As a result of swelling of amide chains, stiffness is increased, capacity of N fibers to resist in additional tensile stresses is improved due to increased fiber to matrix bonding and so is the resistance to impact loading.

Although it differentiates from the previous statement for PVA fibers above and was reported for fibers that were different in length (25 and 50 mm) from the fibers used in this study, there is a counter-view of the effect of fiber length on the impact resistance of concrete material. Mohammadi et al.[55] stated that longer fibers are more effective in arresting the cracks of fibrous concrete due to impact loading. In their study, relatively longer fibers (i.e., 50 mm for that case) were the most effective in arresting the cracks due to impact loading thanks to their superior bond resistance and harder slip out characteristics. Likewise, it is possible to state that the swelling of N fibers upon contact with water and following enhancement in the fiber to matrix bonding which was coupled with the longer length could be one of the reasons

behind the comparable impact performance of ECC with N fibers.

It is also important to mention that impact performance of mixtures produced for this study is very likely to be affected by the dimensions and casting of beam specimens.[56] For instance, the load carrying capacity of a composite material can be increased by 20% when the fiber distribution is altered from random distribution of three-dimensional (3D) to uniform alignment of one-dimensional.[57] Similarly, orientations of fibers, especially those situated in the zone of impact, can be significantly important in modifying the response of flexural impact. Given the very limited cross-sectional area of beam specimens, 50×50 mm^2, tested for impact performance, fibers within the impact zone of ECC specimens are anticipated to be mostly two-dimensional (2D) oriented. In line with the abovementioned statements, specimens with 2D-oriented fibers are expected to perform better in terms of tensile properties and crack bridging capacity in comparison to those with 3D-oriented fibers (e.g., specimens having larger dimensions such as large-scale beams and columns). Utilization of fibers with different characteristics in cementitious systems of ECC is also likely to modify the alignment/orientation of fibers which may change the impact performance, although this requires further clarification with more elaborated tests which are off the coverage of current study.

The most extensively studied mixture of ECC is the PVA fiber-based standard ECC mixture which is also known as Mixture 45 (M45) in the literature[58] (Mixture #25 for this study). Both Tables 3 and 4 make it clear that very close or even better mechanical and impact properties can be obtained from certain ECC mixtures produced with N fibers (e.g., Mixture #19—S1.2–N–0.27). To conclude, results included in the current research show that by properly adjusting the mixture proportions, N fiber-based and relatively cheaper ECC mixtures that are with comparable mechanical and impact resistance properties to that of PVA fiber-based companions can be successfully produced, although further studies are recommended to acquire more cost-effective mixtures greatly outperforming the properties of widely researched ECC mixtures in the open literature.

3.3 | Numerical study

For the comparison of results from the experimental part of the study, in the numerical part, finite element analyses were performed using ABAQUS software.[59] ABAQUS is an advanced finite elements solver capable of modeling and analyzing incremental dynamic problems which is also suitable for examining the effects of sudden impact loading on concrete materials and is widely used by researchers.

As the first step, 3D models of impact test specimens measuring $50 \times 50 \times 750$ mm^3, setup details for impact testing and test conditions were created in the software. By keeping the drop height (600 mm) and mass of steel hammer (9 kg) constant, application of constant impact energy on the specimens was made sure in the software. Since the beam specimens were tested under free fall, no additional force except gravitational force was applied and thus the steel hammer was modeled in a way to move vertically under the sole effect of gravity. Similar support conditions to that of experimental part of the study were considered in the numerical part. To simulate the drop movement of steel hammer under frictional effects in the actual laboratory tests, friction coefficient was defined as 0.20. By this way, results from experimental and numerical studies were compared in a stricter sense.

Before performing the numerical analyses, modeling should be made by using proper element types. For the purposes of current study, elements typed as three dimensional 10-node modified tetrahedrons (C3D10M), which are extensively used in problems related to the impact effects, were utilized in the modeling procedure (Figure 10). After constituting test setup geometry and providing test conditions, material properties were defined in the software. Since stress and deformation values in compression and flexure were obtained in the experimental studies, for numerical analysis, concrete damaged plasticity (CDP) model of ABAQUS software was utilized. CDP model provides a general capability of modeling concrete and uses concepts of isotropic damaged elasticity in combination with isotropic tensile and compressive plasticity to represent the inelastic behavior of concrete as shown in Figure 11. Under uniaxial tension, the stress–strain response follows a linear elastic relationship until reaching to the level of failure stress, σ_{ts}, corresponding to the start of microcracking of concrete. After the failure stress, the formation of microcracks is designed by the strain-softening response. Under uniaxial compression, the response is linear until the level of initial yielding, σ_{c0}. After that point, the responses up to and beyond the ultimate stress

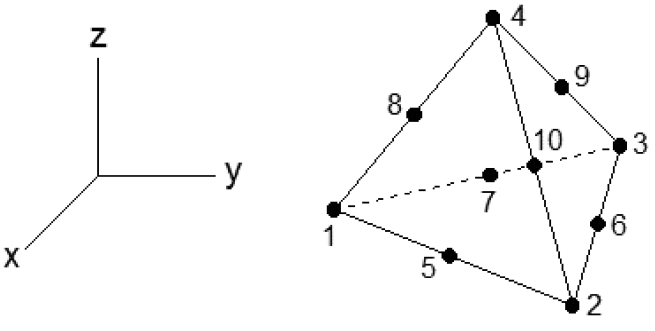

FIGURE 10 C3D10M element type

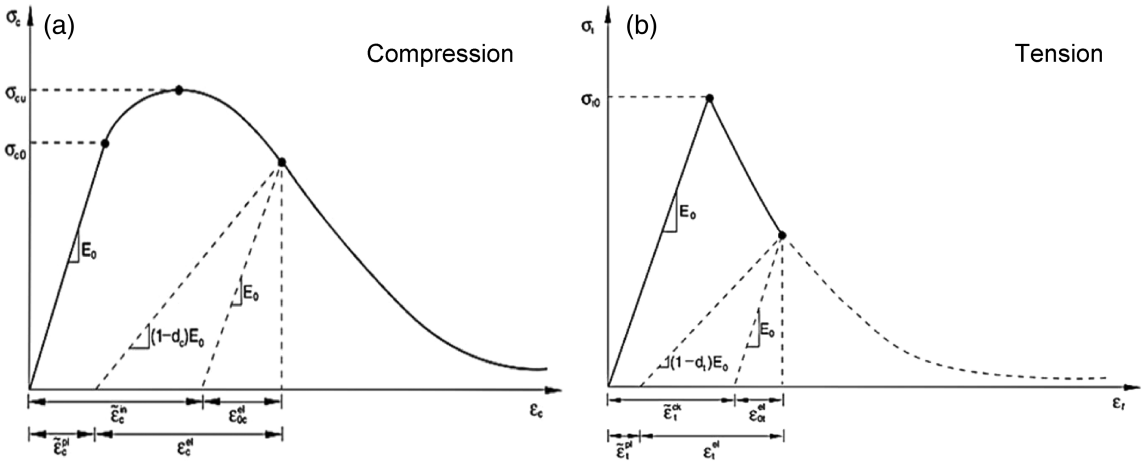

FIGURE 11 Concrete model

level, σ_{cu}, are characterized by strain-hardening and strain-softening, respectively.[59]

Basically, the CDP model is based on plasticity parameters which define the yield surface function, potential flow and viscosity of material along with the compressive and tensile behavior of concrete. These parameters include the dilation angle, flow potential eccentricity, ratio of initial equibiaxial compressive yield stress to initial uniaxial compressive yield stress, a coefficient determining the shape of deviatoric cross section and viscosity parameter represented by ψ, e, σ_{b0}/σ_{c0}, and K_c symbols, respectively. After defining the nonlinear behavior of concrete, material properties of the steel hammer, steel plate, and rubber were assigned to related geometries in the software. Linear elastic material models were used for the steel hammer and plate. The parameters for concrete, steel plate, steel hammer, and rubber are presented in Table 5.

To obtain more reliable results, node numbers were determined after the finite element models of the geometries were divided into small pieces. Time for computation gets longer when smaller finite element sizes are used in the software. Therefore, a specimen from Mixture #1 (FA1.2–0.27) was analyzed for some different element sizes. Finally, size for finite element modeling was decided to be 11.5 mm by considering the time for the analysis and obtained results. Thereby, for the current analysis, the number of nodes and total number of elements were chosen to be 31,885 and 21,846, respectively, for beam specimens with steel plate and rubber layer. On the other hand, the number of nodes and total number of elements were 14,374 and 9,404 for steel hammer, respectively.

TABLE 5 Material properties of concrete, steel plate, hammer, and rubber in the software

Properties	Concrete	Steel hammer and plate	Rubber
Young's modulus (MPa)	24,000	200,000	22
Weight per unit of volume (kg/m^3)	2,400	7,850	1,230
Poisson's ratio	0.20	0.30	0.20
Shear modulus (MPa)	—	76,923	7.59
Bulk modulus (MPa)	—	166,670	73.33
ψ	36	—	—
e	0.01	—	—
σ_{b0}/σ_{c0}	1.16	—	—
K_c	0.667	—	—

The interaction between geometries is also defined in the software. Interaction occurs through contact surfaces in the analyses. Surface to surface contact property was utilized between steel hammer and test specimens. Because impact loading was applied by the hammer on the test specimen, surface of the hammer was defined as the master while the corresponding part of the specimen was defined as slave. The behavior of the contact surfaces was tangential in the software and since the frictions cannot be set to zero during the tests, coefficient of friction was taken as 0.20 in the analyses.

In incremental dynamic analysis, both time steps and time increments were defined from the start to the end of the each drop movement of the hammer. The models were analyzed for short time intervals. Time increments become more important from the beginning of the contact between the hammer and test specimen. Therefore, until the moment of contact, the time increment was 0.0060 s while it was defined as 1.75×10^{-8} s starting from the touch of hammer to the specimen. These increments were repeatedly applied to each one of the specimens until the results were reached.

After completing the nonlinear dynamic analyses for all specimens in the software, acceleration, displacement and impact force results were determined. These results together

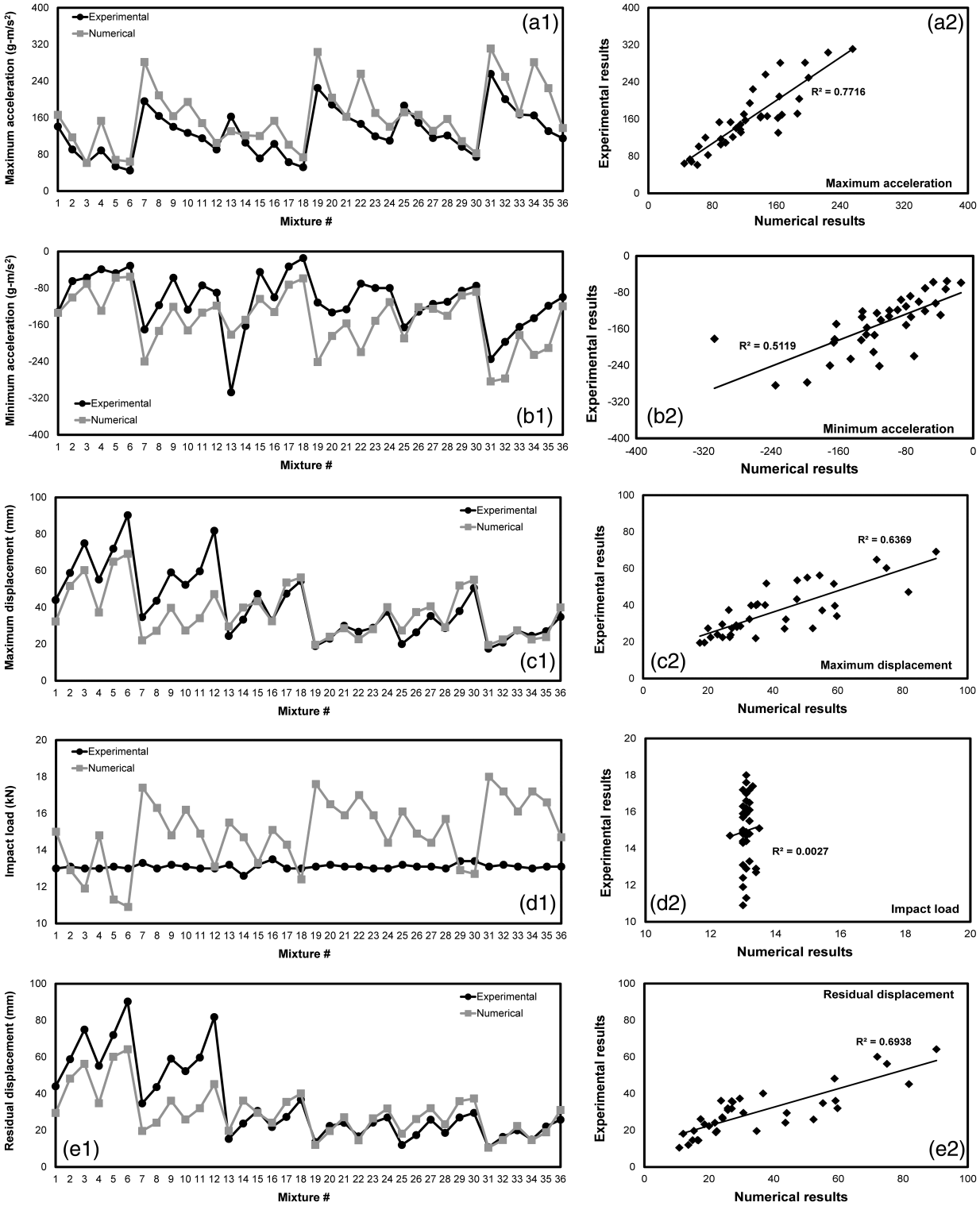

FIGURE 12 Comparison of experimental and numerical test results

with the experimental results were comparatively drawn in Figure 12. von Mises stress distributions which give idea about the crack propagation in test specimens were also obtained after the impact loading was completely transferred to test specimens. These stress distributions with stress values in Pascal (N/m^2) are shown in Figure 13. It can be seen that significant similarities exist between damage occurrences obtained from the experimental program and those obtained from stress contours after numerical analyses.

To have a clearer vision on the comparison of results from different sources, experimental and numerical data were plotted with 1:1 line and coefficient of determination

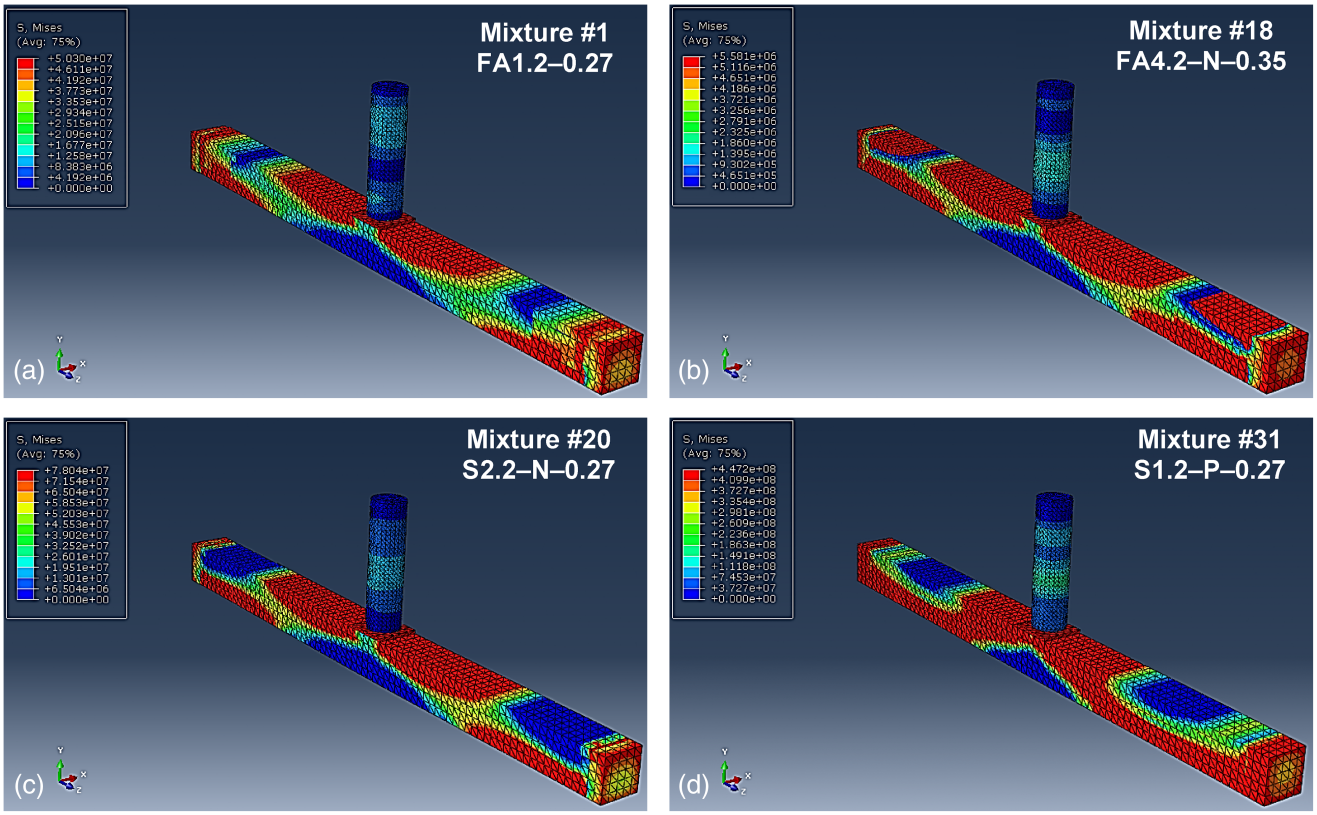

FIGURE 13 Representative von Mises stress distributions for selected mixtures

(R^2) values were calculated (Figure 12). It can be seen from this figure that depending on the impact parameter analyzed, correlation between experimentally and numerically determined parameters showed variations although there was a general correlation trend with maximum and minimum R^2 values of .7716 and .5119 recorded for maximum acceleration and minimum acceleration results, respectively when R^2 value of impact load results was excluded. As Figure 12 makes it clear, R^2 value of experimentally and numerically determined impact load results was found to be relatively small ($R^2 = .0027$). Although results are close to each other, due to relatively close experimental results accumulating around 13.0 kN, they show a nonlinear trend which comes along with very low R^2 value.

Necessary data for the material models of ECC beams analyzed in the numerical part were taken under conditions of static compressive and four-point bending loading performed in the experimental part of the study. Keeping in mind that the data defined for the material models of beams from 36 different ECC beams were acquired only from tests utilized static loading conditions, variations in the experimental and numerical results can be expected. As also detailed in the previous sections and expected, response of concrete materials to slow static and sudden impact loading conditions is different. Moreover, CDP concrete model of ABAQUS finite element software was developed by considering the nonlinear properties of concrete under static loads. It can be considered that observed differences in numerical and experimental results can be due to ABAQUS software not effectively accounting for strain-rate effects. Although such an analysis can be undertaken by different software such as LS-DYNA to complement the drawbacks of ABAQUS, anyhow, it is expected that strain-rate effects will increase the stiffness and resistance which would lead FE analysis results to be always lower than the actual test results which is not the observed case. It can therefore be stated that observed discrepancies especially between numerical and experimental acceleration and displacement results can be related to the complexity of the problem which is subjected to high scatter and difficult to model. More precise results can be attained by further calibration of the model, which does not guarantee good results in future tests, since there is normally more than one way of achieving the same results (more than one way of calibrating). Overall, the authors attribute the observed discrepancy in results to the computer models which are yet with limited ability to accurately predict reality and suggest that further tests on related subject are necessary for developing models of conventional or special concretes (e.g., ECC) under sudden dynamic loads and the developed models should be transferred to the software used.

4 | CONCLUSIONS

In the current research, drop-weight impact performance of ECC manufactured with different mixture parameters were analyzed both experimentally and numerically. Basic mechanical properties of mixtures were also evaluated in terms of compressive strength and flexural properties. ECC mixtures were produced with different types and replacement rates of pozzolanic materials, water to binder ratios, and fiber types. Different pozzolanic materials were Class-F FA and ground granulated blast furnace slag and their rates of replacement with PC were 1.2, 2.2, and 4.2. Different water to binder ratios of ECC were 0.27 and 0.35. Mixtures were produced with PVA or nylon (N) fibers, by 2% of total volume of mixtures. Following are the conclusions drawn from the study:

- Compressive and flexural strength of mixtures were higher when ECC mixtures were produced with slag, lower replacement rates of pozzolanic materials with PC, lower water to cement ratio and fibers. Midspan displacements (ductility) of mixtures improved significantly in the presence of fibers. It was possible to achieve deflection-hardening response for ECC produced with relatively cheaper N fibers by properly adjusting other mixture proportions.
- Between different pozzolanic materials, ECC specimens produced with Class-F FA resulted in worse impact performance compared to those with slag. When the amount of pozzolanic materials increased in the compositions of ECC, reductions in the impact performance were noted. These results were associated with the decrements in the compressive strength results of specimens in general.
- Lower water to binder ratio increased the impact performance of ECC when the other mixture parameters were kept constant. This outcome was also related to the increments in the compressive strength results of mixtures which prevented the specimens from being failed directly from the frontal impact zone.
- Irrespective of the type, fiber addition significantly elevated the impact performance of reference mixtures without fibers. The most significant effect of fibers was to keep the specimens in one piece and to protect their integrity. Although N fibers were used lower in weight (23 kg/m^3) compared to PVA fibers (26 kg/m^3), it was possible to obtain deflection-hardening response under static four-point bending loading and attain comparable resistance capacity to sudden impact loading conditions from ECC mixtures produced with significantly cheaper N fibers.
- Numerical results obtained from ABAQUS were largely concordant with the experimental results. However, some variations were present especially for the experimentally and numerically obtained results of acceleration and displacement since the material models defined for ECC beams were incompatible with sudden dynamic loading conditions. It is suggested that CDP model of ABAQUS finite element software should be improved to obtain more successful and realistic results from ECC-like materials with deflection-hardening capability subjected to effects of sudden impact loading.

ORCID

Gürkan Yıldırım https://orcid.org/0000-0002-3087-0360
Özgür Anıl https://orcid.org/0000-0002-1939-0366
Oğuzhan Şahin https://orcid.org/0000-0003-2104-5761

REFERENCES

1. Padgett J, DesRoches R, Nielson B, et al. Bridge damage and repair costs from hurricane Katrina. J Bridge Eng. 2008;13(1):6–14.
2. El-Tawil S, Severino E, Fonseca P. Vehicle collision with bridge Piers. J Bridge Eng. 2005;10(3):345–353.
3. Eskew E, Jang S. Impacts and analysis for buildings under terrorist attacks. Connecticut, NE: University of Connecticut, (CEE Articles) http://digitalcommons.uconn.edu/cee_articles/1, 2012.
4. Kennedy RP. A review of procedures for the analysis and design of concrete structures to resist missile impact effects. Nucl Eng Des. 1976;37(2):183–203.
5. Ross HE Jr, Sicking DL, Zimmer RA, Michie JD. Recommended procedures for the safety performance evaluation of highway features (no. 350). Washington, DC. Transport Res. 1993; 1–64.
6. Kasan JL, Harries KA, Miller R, Brinkman RJ. Limits of application of externally bonded CFRP repairs for impact-damaged prestressed concrete girders. J Compos Constr. 2014;18(3):A4013013.
7. Sukontasukkul P, Jamnam S, Sappakittipakorn M, Banthia N. Preliminary study on bullet resistance of double-layer concrete panel made of rubberized and steel fiber reinforced concrete. Mater Struct. 2014;47(1–2):117–125.
8. Mindess S, Banthia N, Yan C. The fracture toughness of concrete under impact loading. Cem Concr Res. 1987;17(2):231–241.
9. Ranade R, Li VC, Heard WF, Williams BA. Impact resistance of high strength-high ductility concrete. Cem Concr Res. 2017;98:24–35.
10. Fischer G, Fukuyama H, Li VC. Effect of matrix ductility on the performance of reinforced ECC column members under reversed cyclic loading conditions. Takayama, Japan: DFRCC International Workshop, 2002.
11. Şahmaran M, Li VC. Durability properties of micro-cracked ECC containing high volumes fly ash. Cem Concr Res. 2009;39(11):1033–1043.
12. Alyousif A, Lachemi M, Yıldırım G, Şahmaran M. Effect of self-healing on the different transport properties of cementitious composites. J Adv Concrete Technol. 2015;13(3):112–123.
13. Yıldırım G, Şahmaran M, Balçıkanlı M, Özbay E, Lachemi M. Influence of cracking and healing on the gas permeability of cementitious composites. Construct Build Mater. 2015;85:217–226.

14. Yıldırım G, Şahmaran M, Ahmed HU. Influence of hydrated lime addition on the self-healing capability of high-volume fly ash incorporated cementitious composites. J Mater Civ Eng. 2015;27(6):04014187.
15. Yıldırım G, Keskin ÖK, Keskin SB, Şahmaran M, Lachemi M. A review of intrinsic self-healing capability of engineered cementitious composites: Recovery of transport and mechanical properties. Construct Build Mater. 2015;101:10–21.
16. Şahmaran M, Yıldırım G, Erdem TK. Self-healing capability of cementitious composites incorporating different supplementary cementitious materials. Cem Concr Compos. 2013;35(1):89–101.
17. Şahmaran M, Yıldırım G, Noori R, Özbay E, Lachemi M. Repeatability and pervasiveness of self-healing in engineered cementitious composites. ACI Mater J. 2015;112(4):513–522.
18. Yıldırım G, Aras GH, Banyhussan QS, Şahmaran M, Lachemi M. Estimating the self-healing capability of cementitious composites through non-destructive electrical-based monitoring. NDT E Int. 2015;76:26–37.
19. Yıldırım G, Alyousif A, Şahmaran M, Lachemi M. Assessing the self-healing capability of cementitious composites under increasing sustained loading. Adv Cem Res. 2015;27(10):581–592.
20. Şahmaran M, Yıldırım G, Özbay E, Ahmed K, Lachemi M. Self-healing ability of cementitious composites: Effect of addition of pre-soaked expanded perlite. Mag Concr Res. 2014;66(8):409–419.
21. Şahmaran M, Yıldırım G, Aras GH, Keskin SB, Keskin OK, Lachemi M. Self-healing of cementitious composites to reduce high CO_2 emissions. ACI Mater J. 2017;114(1):93–104.
22. Yıldırım G, Khiavi AH, Yeşilmen S, Şahmaran M. Self-healing performance of aged cementitious composites. Cem Concr Compos. 2018;87:172–186.
23. Li VC. Durable overlay systems with engineered cementitious composites (ECC). Int J Restor Build Monum. 2003;9:215–234.
24. Anıl Ö, Durucan C, Erdem RT, Yorgancılar MA. Experimental and numerical investigation of reinforced concrete beams with variable material properties under impact loading. Construct Build Mater. 2016;125:94–104.
25. Chen Z, Yang Y, Yao Y. Impact properties of engineered cementitious composites with high volume fly ash using SHPB test. J Wuhan Univ Technol. 2012;27(3):590–596.
26. Yang EH, Li VC. Tailoring engineered cementitious composites for impact resistance. Cem Concr Res. 2012;42(8):1066–1071.
27. Li VC, Mishra DK, Wu HC. Matrix design for pseudo-strain-hardening fibre reinforced cementitious composites. Mater Struct. 1995;28(10):586–595.
28. Demirhan S, Yıldırım G, Banyhussan QS, et al. Impact behaviour of nano-modified deflection-hardening fibre reinforced concretes. Mag Concr Res. 2019;1–46. https://doi.org/10.1680/jmacr.18.00541.
29. Yıldırım G. Dimensional stability of deflection-hardening hybrid fiber reinforced concretes with coarse aggregate: Suppressing restrained shrinkage cracking. Struct Con. 2018;20:836–850. https://doi.org/10.1002/suco.201800096.
30. Al-Najjar Y, Yeşilmen S, Al-Dahawi AM, et al. Physical and chemical actions of nano-mineral additives on properties of high-volume fly ash engineered cementitious composites. ACI Mater J. 2016;113(6):791–801.
31. Yeşilmen S, Al-Najjar Y, Balav MH, Şahmaran M, Yıldırım G, Lachemi M. Nano-modification to improve the ductility of cementitious composites. Cem Concr Res. 2015;76:170–179.
32. Tosun-Felekoğlu K, Gödek E, Keskinateş M, Felekoğlu B. Utilization and selection of proper fly ash in cost effective green HTPP-ECC design. J Clean Prod. 2017;149:557–568.
33. Felekoğlu B, Tosun-Felekoğlu K, Keskinateş M, Gödek E. A comparative study on the compatibility of PVA and HTPP fibers with various cementitious matrices under flexural loads. Construct Build Mater. 2016;121:423–428.
34. Snoeck D, De Belie N. Mechanical and self-healing properties of cementitious composites reinforced with flax and cottonised flax, and compared with polyvinyl alcohol fibres. Biosyst Eng. 2012;111(4):325–335.
35. Snoeck D, Smetryns PA, De Belie N. Improved multiple cracking and autogenous healing in cementitious materials by means of chemically-treated natural fibres. Biosyst Eng. 2015;139:87–99.
36. Banyhussan QS, Yıldırım G, Bayraktar E, Demirhan S, Şahmaran M. Deflection-hardening hybrid fiber reinforced concrete: The effect of aggregate content. Construct Build Mater. 2016;125:41–52.
37. Banyhussan QS, Yıldırım G, Anıl Ö, Erdem RT, Ashour A, Şahmaran M. Impact resistance of deflection-hardening fiber reinforced concretes with different mixture parameters. Struct Con. 2019;20:1036–1050. https://doi.org/10.1002/suco.201800233.
38. Demir İ, Sevim Ö, Tekin E. The effects of shrinkage-reducing admixtures used in self-compacting concrete on its strength and durability. Construct Build Mater. 2018;172:153–165.
39. Ahmed SFU, Maalej M, Paramasivam P. Flexural responses of hybrid steel—Polyethylene fiber reinforced cement composites containing high volume fly ash. Construct Build Mater. 2007;21:1088–1097.
40. Wang S, Li VC. Engineered cementitious composites with high-volume fly ash. ACI Mater J. 2007;104(3):233–241.
41. Ahmed SFU. Deflection hardening behaviour of short fibre reinforced fly ash based geopolymer composites. Mater Des. 2013;50:674–682.
42. Nataraja MC, Nagaraj TS, Basavaraja SB. Reproportioning of steel fibre reinforced concrete mixes and their impact resistance. Cem Concr Res. 2005;35(12):2350–2359.
43. Nili M, Afroughsabet V. Combined effect of silica fume and steel fibers on the impact resistance and mechanical properties of concrete. Int J Impact Eng. 2010;37(8):879–886.
44. Nili M, Afroughsabet V. The effects of silica fume and polypropylene fibers on the impact resistance and mechanical properties of concrete. Construct Build Mater. 2010;24(6):927–933.
45. Atahan HN, Pekmezci BY, Tuncel EY. Behavior of PVA fiber-reinforced cementitious composites under static and impact flexural effects. J Mater Civ Eng. 2013;25(10):1438–1445.
46. Zhang L. Impact resistance of high strength fiber reinforced concrete. [doctoral dissertation]. University of British Columbia; 2008.
47. Wang S, Le HTN, Poh LH, Feng H, Zhang MH. Resistance of high-performance fiber-reinforced cement composites against high-velocity projectile impact. Int J Impact Eng. 2016;95:89–104.
48. Mao L, Barnett SJ, Tyas A, Warren J, Schleyer GK, Zaini SS. Response of small scale ultra high performance fibre reinforced

concrete slabs to blast loading. Construct Build Mater. 2015;93: 822–830.
49. Barnett S, Millard S, Tyas A, Schleyer G. Briefing: Blast tests of fibre-reinforced concrete panels. Proc ICE Constr Mater. 2010;163 (3):127–129.
50. Clifton JR. Penetration resistance of concrete: A review. Vol NBS Special Publication 480-45. Springfield, VA: National Technical Information Service, 1982.
51. Zhang MH, Shariff MSH, Lu G. Impact resistance of high-strength fibre-reinforced concrete. Mag Concr Res. 2007;59(3): 199–210.
52. Song PS, Hwang S, Sheu BC. Strength properties of nylon- and polypropylene-fiber-reinforced concretes. Cem Concr Res. 2005; 35(8):1546–1550.
53. FGJ Harold RWJ, John MMIII. Eldridge. Extrusion: The definitive processing guide and handbook. New York, NY: William Andrew, 2005.
54. Yap SP, Alengaram UJ, Jumaat MZ. Enhancement of mechanical properties in polypropylene–and nylon–fibre reinforced oil palm shell concrete. Mater Des. 2013;49:1034–1041.
55. Mohammadi Y, Carkon-Azad R, Singh SP, Kaushik SK. Impact resistance of steel fibrous concrete containing fibres of mixed aspect ratio. Construct Build Mater. 2009;23(1):183–189.
56. Ranade R. Advanced cementitious composite development for resilient and sustainable infrastructure. [doctoral dissertation]. University of Michigan: Ann Arbor; 2014.
57. Cox HL. The elasticity and strength of paper and other fibrous materials. Bri J Appl Phys. 1952;122(1):10–18.
58. Şahmaran M, Li VC. Durability of mechanically loaded engineered cementitious composites under highly alkaline environments. Cem Concr Compos. 2008;30(2):72–81.
59. ABAQUS User's Manual, Version 6.12, SIMULIA, Dassault Systèmes Simulia Corp., 2015.

AUTHOR BIOGRAPHIES

Gürkan Yıldırım, Department of Civil Engineering
Kırıkkale University
Kırıkkale, Turkey
gyildirim@kku.edu.tr

Farhad Emami Khiavi, Department of Civil Engineering
Gazi University
Ankara, Turkey
farhademami69@yahoo.com

Özgür Anıl, Department of Civil Engineering
Gazi University
Ankara, Turkey
oanil@gazi.edu.tr

Oğuzhan Şahin, Department of Civil Engineering
Kırşehir Ahi Evran University
Kırşehir, Turkey
oguzhansahin@ahievran.edu.tr

Mustafa Şahmaran, Department of Civil Engineering
Hacettepe University
Ankara, Turkey
sahmaran@hacettepe.edu.tr

Recep Tuğrul Erdem, Department of Civil Engineering
Manisa Celal Bayar University
Manisa, Turkey
tugrul.erdem@bayar.edu.tr

How to cite this article: Yıldırım G, Khiavi FE, Anıl Ö, Şahin O, Şahmaran M, Erdem RT. Performance of engineered cementitious composites under drop-weight impact: Effect of different mixture parameters. *Structural Concrete*. 2020;21:1051–1070. https://doi.org/10.1002/suco.201900125